ISSN 1330-3651 (Print), ISSN 1848-6339 (Online)
https://doi.org/10.17559/TV-20200716182721
Original scientific paper

Thermodynamic Analysis of CO_2 Closed-Cycle Gas Turbine for Marine Applications at Various Pressure Ratios

Vedran MRZLJAK*, Daniel ŠTIFANIĆ, Hrvoje MEŠTRIĆ, Zlatan CAR

Abstract: A thermodynamic analysis of CO_2 closed-cycle gas turbine is presented in this paper. Two processes are investigated - base process and the same process upgraded with a heat regenerator. Maximum specific useful work is 159.94 kJ/kg for both observed processes. Involving of heat regenerator inside base CO_2 closed-cycle gas turbine process requires attention due to required temperature differences - high pressure ratios cannot be obtained with a high efficiency heat regenerator. Base CO_2 closed-cycle gas turbine process did not reach cycle efficiency higher than 25%, while for the upgraded process the cycle efficiency can reach 40% at high pressure ratio and for high regenerator efficiency. Additionally, multilayer perceptron is trained in order to achieve high quality models for estimating specific useful work and efficiency for both, base and upgraded process. As a result, MLP with three hidden layers achieved high values of R^2 score.

Keywords: closed-cycle gas turbine; CO_2; machine learning; multilayer perceptron; thermodynamic analysis; various pressure ratios

1 INTRODUCTION

Nowadays, in the marine propulsion, diesel engine prevails [1-3]. Steam propulsion plants are rarely used (while taking into account the entire world fleet), but are still dominant in the propulsion of the LNG (Liquefied Natural Gas) carriers due to many specificities of such ships as well as due to the specificity of transported cargo [4, 5]. Gas turbines are usually part of complex ship propulsion systems which consist of many various elements [6, 7].

Gas turbines are characteristic elements due to the fact that the amount of heat as well as the temperature of combustion gases which remains after the expansion inside a gas turbine (waste heat) is much higher in comparison to other propulsion elements. This fact is the main reason why the gas turbines are unavoidable elements of combined-cycle power plants [8, 9]. High temperature and high heat amount of combustion gases after the gas turbine are the main elements why the engineers and researchers are intensively involved in the development of various waste heat recovery systems which will increase the efficiency (and simultaneously decrease losses) in power systems where the gas turbines are the constituent components [10].

In this paper is presented a thermodynamic analysis of CO_2 closed-cycle gas turbine which operates by using a waste heat (waste heat is delivered from gas turbine combustion gases). Two processes are investigated - base process and the same process upgraded with a heat regenerator. Analysis of various operating parameters for both observed processes is performed at different pressure ratios. Obtained cycle efficiency of the analyzed CO_2 closed-cycle gas turbine shows that the operation of this process can be beneficial only by using a heat regenerator. Moreover, authors use a machine learning technique in order to estimate output parameters of CO_2 closed-cycle gas turbine. First, the obtained data will be rearranged, second, the multilayer perceptron (MLP) algorithm will be trained with prepared data and the performance of each model will be evaluated using Coefficient of determination (R^2). Afterwards, the obtained result of each model will be compared.

2 DESCRIPTION AND OPERATING CHARACTERISTICS OF THE ANALYZED CO_2 CLOSED-CYCLE GAS TURBINE (BASE PROCESS AND UPGRADED PROCESS)

Scheme of the base CO_2 closed-cycle gas turbine process is presented in Fig. 1a [11]. Turbocompressor increases CO_2 pressure and delivers it to the heater. In the heater, CO_2 is heated by combustion gases from gas turbine and in such way, it is prepared for expansion in a gas turbine. After the heater, CO_2 has the highest temperature inside the whole CO_2 closed-cycle gas turbine process and expands through the gas turbine, after which it is delivered to the cooler. The cooler decreases CO_2 temperature (regardless of used cooling medium) and after the cooler, CO_2 with a decreased temperature is delivered to turbocompressor again. Turbocompressor increases the CO_2 pressure (and simultaneously CO_2 temperature) after which the whole process is continuously repeated.

Fig. 1b presents CO_2 closed-cycle gas turbine process upgraded with a heat regenerator. Heat regenerator is a CO_2-CO_2 heat exchanger in which CO_2 after expansion inside the turbine (CO_2 of higher temperature) is used for heating CO_2 after turbocompressor (CO_2 of lower temperature). Regenerator operation did not influence turbocompressor or the turbine, but it notably reduced heat amount required for the CO_2 heating in the heater and simultaneously, notably reduced the amount of cooling medium required for a CO_2 cooling purposes in the cooler. Therefore, inside the regenerator is usefully applied one part of CO_2 heat amount which will be released from the process in the cooler if the gas turbine does not possess regenerator (base process, Fig. 1a).

For both observed processes (base or upgraded), instead of combustion gases from the gas turbine, in the heater can be used any heat from any heat source. Also, in the cooler can be used any allowable cooling medium for CO_2 temperature decrease (both observed processes).

The most common usage of both observed CO_2 closed-cycle gas turbine processes (base or upgraded) is in driving an electrical generator and producing additional electrical power, as presented in Fig. 1 [12].

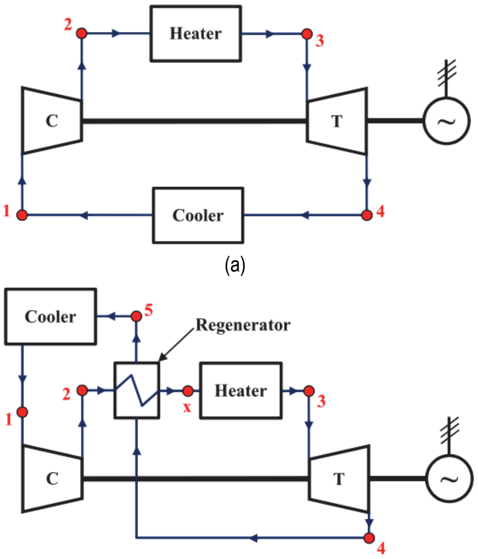

(a)

(b)

Figure 1 Scheme of the CO_2 closed-cycle gas turbine with marked operating points required for the analysis: (a) Base process; (b) Process with the regenerator

It should be noted for both observed CO_2 closed-cycle gas turbine processes that they operate between two pressures - lower pressure at the turbocompressor inlet (gas turbine outlet) and higher pressure at the turbocompressor outlet (gas turbine inlet), Fig. 2. Pressure ratio (higher/lower pressure) is an important operating parameter of both observed CO_2 closed-cycle gas turbine processes.

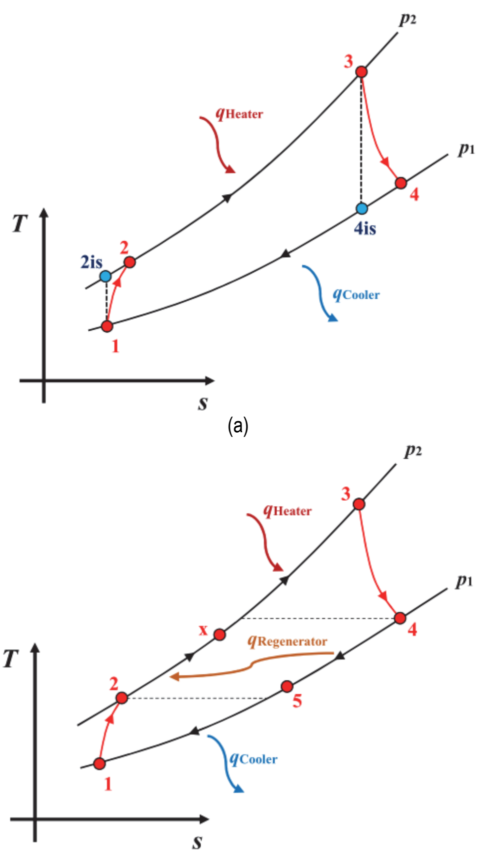

(a)

(b)

Figure 2 *T-s* diagrams of the CO_2 closed-cycle gas turbine with marked operating points required for the analysis: (a) Base process; (b) Process with the regenerator

In Fig. 2, for both observed processes, operating points are marked in relation to Fig. 1. Due to analysis simplicity, for both observed processes (base and upgraded), the pressure drops inside the heater, cooler and regenerator which occur in the real operation are neglected, Fig. 2.

T-s diagram of the base CO_2 closed-cycle gas turbine process is presented in Fig. 2a. In Fig. 2a are also presented ideal and real thermodynamic processes of turbocompressor and gas turbine. A comparison of real and ideal thermodynamic processes defines the isentropic efficiency of turbocompressor and gas turbine. Ideal (isentropic) process assumes always the same CO_2 specific entropy.

T-s diagram of the CO_2 closed-cycle gas turbine process upgraded with a heat regenerator is presented in Fig. 2b. One part of heat from the CO_2 after the expansion process (operating points 4-5) is transferred to CO_2 after the turbocompressor (operating points 2-x). In such way, the amount of heat delivered in the heater is notably reduced (operating points x-3) in comparison to the base process where heat delivery in the heater occurs between operating points 2-3. Simultaneously, such heat transfer will decrease the amount of heat released from the process in the cooler. Also, Fig. 2b clearly shows that heat regenerator did not have any influence on the turbocompressor and gas turbine operation.

3 EQUATIONS FOR THE CO_2 CLOSED-CYCLE GAS TURBINE THERMODYNAMIC ANALYSIS

All the equations for the CO_2 closed-cycle gas turbine analysis (both base and upgraded processes) are defined according to operating points presented in Fig. 1 and Fig. 2.

3.1 Equations for the Base CO_2 Closed-Cycle Gas Turbine Process

In the base CO_2 closed-cycle gas turbine process, CO_2 specific enthalpy after compression in the turbocompressor is calculated by using equation for turbocompressor isentropic efficiency:

$$\eta_{\mathrm{TC,is}} = \frac{h_{2\mathrm{is}} - h_1}{h_2 - h_1} \tag{1}$$

where h is operating medium (CO_2) specific enthalpy in kJ/kg. Specific work of turbocompressor (in kJ/kg) is:

$$w_{\mathrm{TC}} = h_2 - h_1 \tag{2}$$

Specific heat (in kJ/kg) transferred to operating medium (CO_2) in the heater is calculated as:

$$q_{\mathrm{Heater}} = h_3 - h_2 \tag{3}$$

CO_2 specific enthalpy after expansion in the turbine is calculated by using the equation for turbine isentropic efficiency:

$$\eta_{\mathrm{TU,is}} = \frac{h_3 - h_4}{h_3 - h_{4\mathrm{is}}} \tag{4}$$

Specific work of the turbine (in kJ/kg) is:

$$w_{\mathrm{TU}} = h_3 - h_4 \tag{5}$$

The specific useful work of the whole process (in kJ/kg) is:

$$w_{\mathrm{Useful}} = w_{\mathrm{TU}} - w_{\mathrm{TC}} \tag{6}$$

The efficiency of the whole cycle is:

$$\eta_{\mathrm{Cycle}} = \frac{w_{\mathrm{Useful}}}{q_{\mathrm{Heater}}} = \frac{w_{\mathrm{Useful}}}{h_3 - h_2} \tag{7}$$

Pressure ratio, for both observed processes (based and upgraded) is defined as:

$$\beta = \frac{p_2}{p_1} = \frac{p_3}{p_4} \tag{8}$$

with a note that for the base process is valid:

$$p_2 = p_{2\mathrm{is}} = p_3 \tag{9}$$

$$p_1 = p_{4\mathrm{is}} = p_4 \tag{10}$$

while for the process upgraded with a heat regenerator is valid:

$$p_2 = p_{2\mathrm{is}} = p_{\mathrm{x}} = p_3 \tag{11}$$

$$p_1 = p_5 = p_{4\mathrm{is}} = p_4 \tag{12}$$

3.2 Equations for the CO_2 Closed-Cycle Gas Turbine Process Upgraded with the Regenerator

As mentioned before, heat regenerator involved in the CO_2 closed-cycle gas turbine process did not have any influence on turbocompressor operation.

Specific heat (in kJ/kg) transferred to colder CO_2 (after the turbocompressor) in the heat regenerator, for the upgraded process (R is the mark for the process with the heat regenerator), is:

$$q_{\mathrm{CO_2,TC,R}} = h_{\mathrm{x}} - h_2 \tag{13}$$

Specific heat (in kJ/kg) transferred to operating medium (CO_2) in the heater for the upgraded process is:

$$q_{\mathrm{Heater,R}} = h_3 - h_{\mathrm{x}} \tag{14}$$

For the upgraded process, CO_2 specific enthalpy after expansion in the turbine and specific work of the turbine are calculated by using the same equations as in base process (Eq. (4) and Eq. (5)), because heat regenerator did not have any influence on the turbine operation.

Specific heat (in kJ/kg) transferred from hotter CO_2 (after the turbine) in the heat regenerator, for the upgraded process, is:

$$q_{\mathrm{CO_2,TU,R}} = h_4 - h_5 \tag{15}$$

Heat regenerator efficiency (Reff in the Figures) is a ratio of heat amount transferred to colder CO_2 (after the turbocompressor) and heat amount which can be transferred to colder CO_2 in an ideal situation:

$$\eta_{\mathrm{R}} = \frac{h_{\mathrm{x}} - h_2}{h_4 - h_2} \tag{16}$$

The specific useful work of the whole upgraded process is calculated with an identical equation as in the base process (Eq. (6)).

The efficiency of the whole cycle upgraded with a heat regenerator is:

$$\eta_{\mathrm{Cycle,R}} = \frac{w_{\mathrm{Useful}}}{q_{\mathrm{Heater,R}}} = \frac{w_{\mathrm{Useful}}}{h_3 - h_{\mathrm{x}}} \tag{17}$$

4 CO_2 PROPERTIES REQUIRED FOR THE ANALYSIS (BASE AND UPGRADED PROCESS)

Main input data for both CO_2 closed-cycle gas turbine processes are derived from the recommendations of Dragunov [13]. CO_2 properties in each operating point presented in Fig. 1 and Fig. 2 are calculated by using NIST REFPROP 9.0 software [14].

4.1 Main Input Data and Procedure of Properties Calculation for Both Processes (Base and Upgraded)

The input data for the base process (starting with turbocompressor inlet) are:

- CO_2 pressure and temperature at the turbocompressor inlet are 7.7 MPa and 32 °C,
- pressure ratio is varied in this analysis from 1.3 up to 20 for a base process and from 1.3 up to 6 for the upgraded process,
- CO_2 in operating point 2 (Fig. 2) has the same specific entropy as in the operating point 1,
- for all the calculations performed in this paper, turbocompressor isentropic efficiency (Eq. (1)) and turbine isentropic efficiency (Eq. (4)) are the same and equal to 90% (as recommended in [13]),
- CO_2 specific enthalpy after real (polytropic) compression process (operating point 2) is calculated by using the equation for turbocompressor isentropic efficiency (as the pressure in operating point 2 is known, from CO_2 pressure and specific enthalpy are calculated all the other properties in operating point 2),
- in operating point 3, CO_2 temperature is 505 °C as recommended in [13],
- operating point 4 (Fig. 2) has the same CO_2 specific entropy as operating point 3,

- specific enthalpy in operating point 4 is calculated from the equation of turbine isentropic efficiency (Eq. (4)).

The input data for the process upgraded with a heat regenerator are:

- temperature and pressure at the turbocompressor inlet as well as the temperature at the turbine inlet are identical as in the base process,
- CO_2 properties in operating points 2, 2, 4 and 4 are calculated by following the same principles as in the base process (turbocompressor and turbine isentropic efficiencies are also 90%),
- CO_2 specific enthalpy in operating point x (Fig. 1b) and Fig. 2b) is calculated by using the equation for heat regenerator efficiency (Eq. (16)). Heat regenerator efficiencies are varied in this analysis from 40% up to 60% (selected range of heat regenerator efficiencies is further explained during the obtained results presentation),
- CO_2 specific enthalpy in operating point 5 (Fig. 1b and Fig. 2b) is calculated by equalizing Eq. (13) and Eq. (15).

4.2 Example of CO_2 Properties in the Base and Upgraded Processes

For the base CO_2 closed-cycle gas turbine process, CO_2 properties in each operating point from Fig. 1a and Fig. 2a are presented in Tab. 1 for the pressure ratio equal to 3.

Table 1 CO_2 properties in each operating point of the base process

Operating Point*	Temperature / °C	Pressure / MPa	Specific enthalpy / kJ/kg	Specific entropy / kJ/kg·K
1	32.00	7.7	306.23	1.3463
2is	64.71	23.1	328.73	1.3463
2	65.79	23.1	331.23	1.3537
3	505.00	23.1	976.94	2.6402
4is	366.28	7.7	828.94	2.6402
4	379.15	7.7	843.74	2.6631

* Operating point numeration refers to Fig. 1a and Fig. 2a

For the CO_2 closed-cycle gas turbine process upgraded with a heat regenerator, CO_2 properties in each operating point from Fig. 1b and Fig. 2b are presented in Tab. 2 for the pressure ratio equal to 4 and for the heat regenerator efficiency equal to 50%.

Table 2 CO_2 properties in each operating point of the process upgraded with a heat regenerator

Operating Point*	Temperature / °C	Pressure / MPa	Specific enthalpy / kJ/kg	Specific entropy / kJ/kg·K
1	32.00	7.7	306.23	1.3463
2is	74.76	30.8	338.88	1.3463
2	76.53	30.8	342.51	1.3567
3	505.00	30.8	971.40	2.5763
4is	331.51	7.7	789.20	2.5763
4	347.48	7.7	807.42	2.6060
x	204.31	30.8	574.96	1.9281
5	142.79	7.7	574.96	2.1512

* Operating point numeration refers to Fig. 1b and Fig. 2b

According to data presented in Tab. 1 and Tab. 2, it should be highlighted that both of the observed processes are supercritical ones. Supercritical fluid (in this case CO_2) is a fluid at a temperature and pressure above its critical point, where distinct liquid and gas phases do not exist. In the literature can be found that the thermal efficiency of such processes is higher in comparison to other similar processes for the heat source temperatures range from 450 °C to 700 °C [12, 13]. That was the main reason why supercritical processes are selected for the analysis.

5 MACHINE LEARNING APPROACH FOR CO_2 CLOSED-CYCLE GAS TURBINE OUTPUT PARAMETER ESTIMATION

In order to create models capable of estimating specific useful work and efficiency of the CO_2 closed-cycle gas turbine process, machine learning algorithm, precisely MLP can be used. This section provides a brief overview of MLP and evaluation criteria as well as description of the grid search algorithm.

5.1 Dataset Description

Data described in section 4. are used to create the dataset appropriate for MLP regressor. As input data for the base and upgraded processes, CO_2 properties in each operating point are used. In the case of the upgraded process, data are obtained for the various efficiency of heat regenerator. For each combination of input data, belonging specific useful work and efficiency of the whole process are added. Finally, the dataset for base process consists of 660 data-points while the dataset for upgraded process consists of 1364 data-points. Each of datasets is divided into two parts with the train-test distribution of 70% : 30%.

5.2 Multilayer Perceptron

Multilayer perceptron (MLP) is a class of deep, artificial neural network (ANN) which consists of multiple layers of interconnected neurons [15]. Each layer of neurons is connected by weights to the neurons of the subsequent layer. Furthermore, between the input and the output layer can exist one or more hidden layers which allows capturing very complex relationships between input and output variables. Training process can be considered as adjusting the parameters of the model i.e. weights and biases with the goal of minimizing a cost function. Since the MLP without activation function can perform linear mappings only, applying activation function to the layers can add non-linear property allowing the model to approximate highly non-linear functions [15]. Commonly used activation functions are ReLU, Sigmoid, Tanh and Identity.

In order to evaluate the performance of the obtained model, coefficient of determination (R^2) is utilized. It can be described as a statistical measure which is defined in the range between 0.0 and 1.0, where a value of 1.0 represents a perfect fit of the model and vice-versa [16]. R^2 can be calculated as follows:

$$R^2 = 1 - \frac{S_{\mathrm{res}}}{S_{\mathrm{tot}}} = 1 - \frac{\sum_i \left(y_i - \hat{y}_i\right)^2}{\sum_i \left(y_i - \bar{y}\right)^2} \tag{18}$$

where S_{res} represents the residual sum of squares and S_{tot} represents the total sum of squares. Furthermore, y_i is the true data, $\hat{y}_i$ is predicted data and $\bar{y}$ represents the mean of all observed true data.

5.3 Hyperparameter Optimization

MLP architecture is described with numerous hyperparameters that can be optimized in order to achieve high regression performance. Utilizing the grid search algorithm, optimal combination of MLP hyperparameters can be determined [17].

Table 3 Possible combinations of hyperparameter values used to train MLP models

Hyperparameter	Parameter value
Number of hidden layers	1, 2, 3, 4
Number of neurons per layer	8, 16, 32
Activation function	ReLU, Sigmoid, Tanh, Identity
Optimizer	SGD, Adam, RMSprop
Learning rate	$1e^{-2}$, $1e^{-3}$
Learning rate decay	$1e^{-5}$, $1e^{-6}$, $1e^{-7}$
Regularization parameter - *L2*	$1e^{-3}$, $1e^{-4}$, $1e^{-5}$

The first step is to manually define a search space i.e. to define all possible parameter combinations which can, theoretically, give the best model performance. Second step is to build the model for each hyperparameter combination possible and store the performance value. In the last step, hyperparameters of the MLP model that achieves the highest regression performance are used for further testing. In this research adjusted hyperparameters are number of hidden layers, number of neurons per hidden layer, type of activation function, optimizer, learning rate, learning rate decay, and regularization parameter *L*2. The possible values of hyperparameters used in training process are shown in Tab. 3.

6 RESULTS AND DISCUSSION

The change of turbocompressor, turbine and specific useful work for the analyzed CO_2 closed-cycle gas turbine process during the change in pressure ratio is presented in Fig. 3. The change of all parameters presented in Fig. 3 is valid for both analyzed CO_2 closed-cycle gas turbine processes (base and upgraded) because a heat regenerator addition into the process did not have any influence on the turbocompressor or turbine operation.

An increase in pressure ratio continuously increases both turbocompressor and turbine specific work and vice versa. However, the difference between specific work of turbine and turbocompressor (specific useful work) during the pressure ratio increase, continuously increases (for the selected CO_2 operating parameters, Tab. 1 and Tab. 2) only till the pressure ratio reaches value of 12. At pressure ratio equal to 12 both CO_2 closed-cycle gas turbine processes will develop the highest specific useful work equal to 159.94 kJ/kg. A further increase in pressure ratio (higher than 12) will result with a decrease in specific useful work.

In [13] it can be found that the pressure ratios recommended for observed processes operation (according to selected CO_2 operating parameters, Tab. 1 and Tab. 2) are between 2 and 4, which is also marked in Fig. 3.

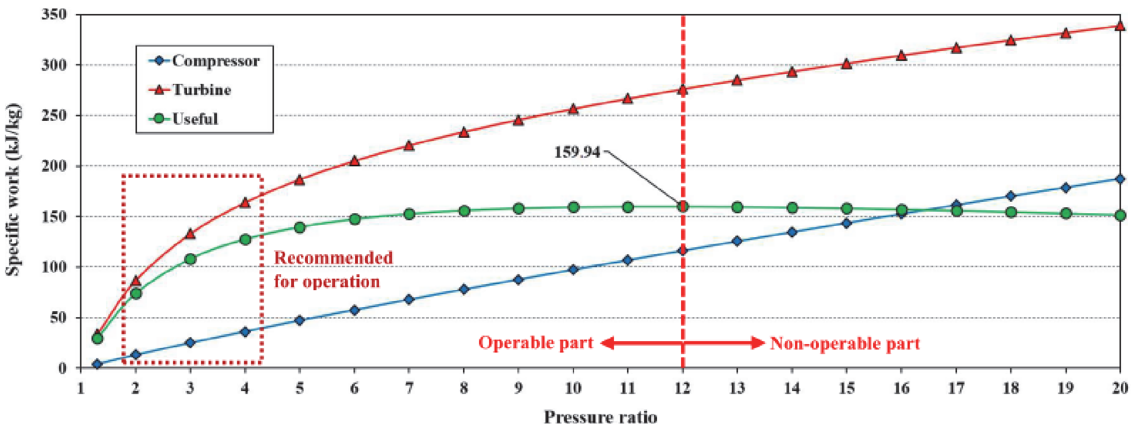

Figure 3 Specific work of turbocompressor, turbine and useful work of the CO_2 closed-cycle gas turbine at various pressure ratios (valid for both analyzed processes)

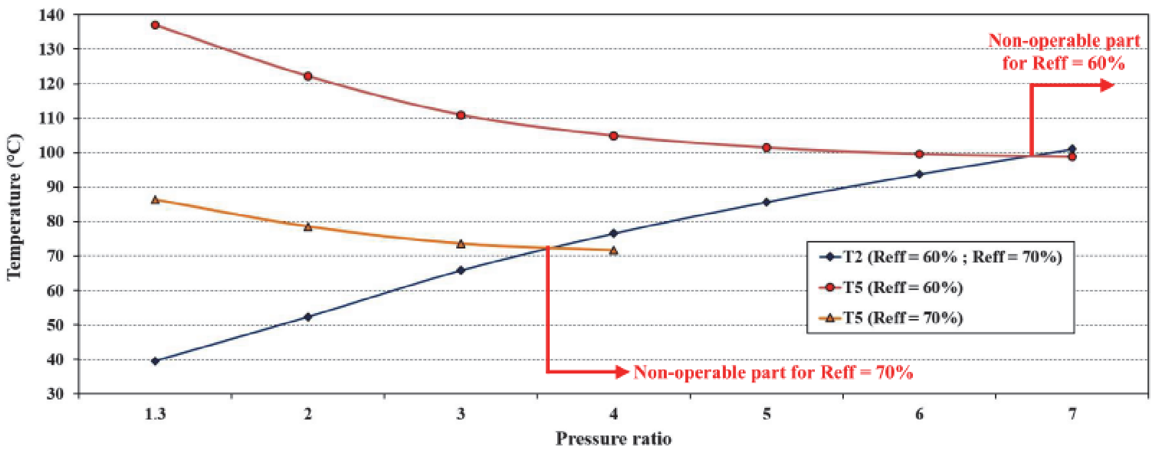

Figure 4 The relation between temperatures *T*2 and *T*5 - definition of observed regenerator efficiency range

Heat regenerator efficiency (Reff in the Figures) is defined by Eq. (16). As the heat regenerator is a CO_2-CO_2 heat exchanger [18], during its operation should be ensured sufficient heat amount (from hotter CO_2 after the turbine to colder CO_2 after the turbocompressor) as well as sufficient temperature differences. Considering Fig. 2b, for the proper heat exchange inside the heat regenerator, it should be ensured that CO_2 after the turbine (operating point 4) has always higher temperature than CO_2 at the heater inlet (operating point x), while at the same time it should be ensured that the CO_2 temperature at the cooler inlet (operating point 5) is always higher than the CO_2 temperature at the turbocompressor outlet.

According to selected CO_2 operating parameters (Tab. 2), one interesting fact occurs for the process upgraded with a heat regenerator, which is presented in Fig. 4. The CO_2 temperature at the turbocompressor outlet ($T2$) continuously increases with an increase in pressure ratio. At the same time, the CO_2 temperature at the cooler inlet ($T5$) continuously decreases with a pressure ratio increase. Heat regenerator with higher efficiency will have lower CO_2 temperatures at the cooler inlet, Fig. 4. The problem with heat regenerator of high efficiency is that the CO_2 temperature at the cooler inlet ($T5$) will reach CO_2 temperature after the turbocompressor ($T2$) for low pressure ratios - further increase in pressure ratio will disable proper heat regenerator operation, Fig. 4.

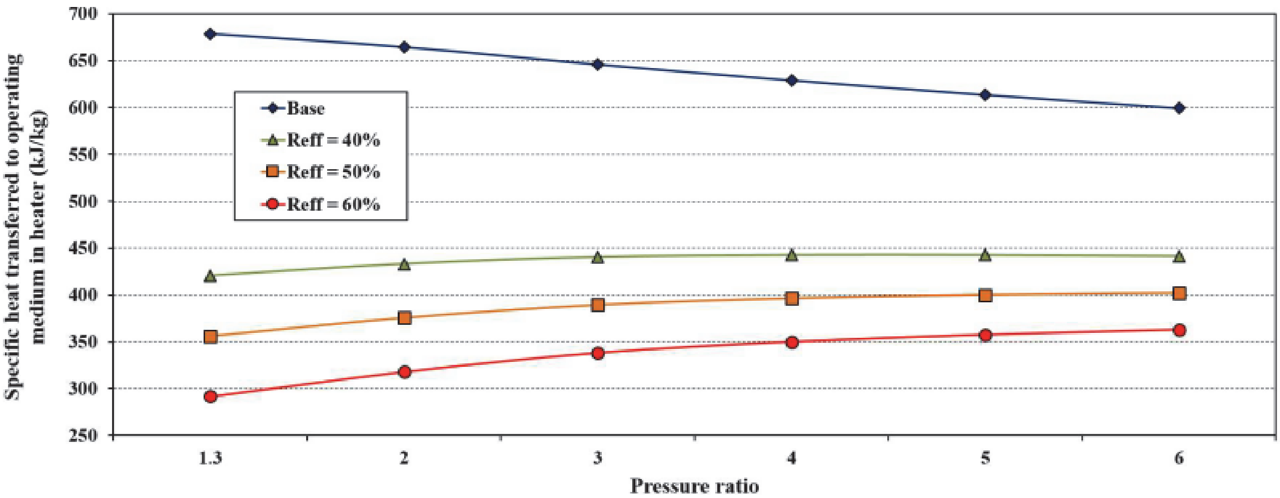

Figure 5 Specific heat transferred to operating medium (CO_2) in the heater for the base process and for the process with regenerator at various pressure ratios

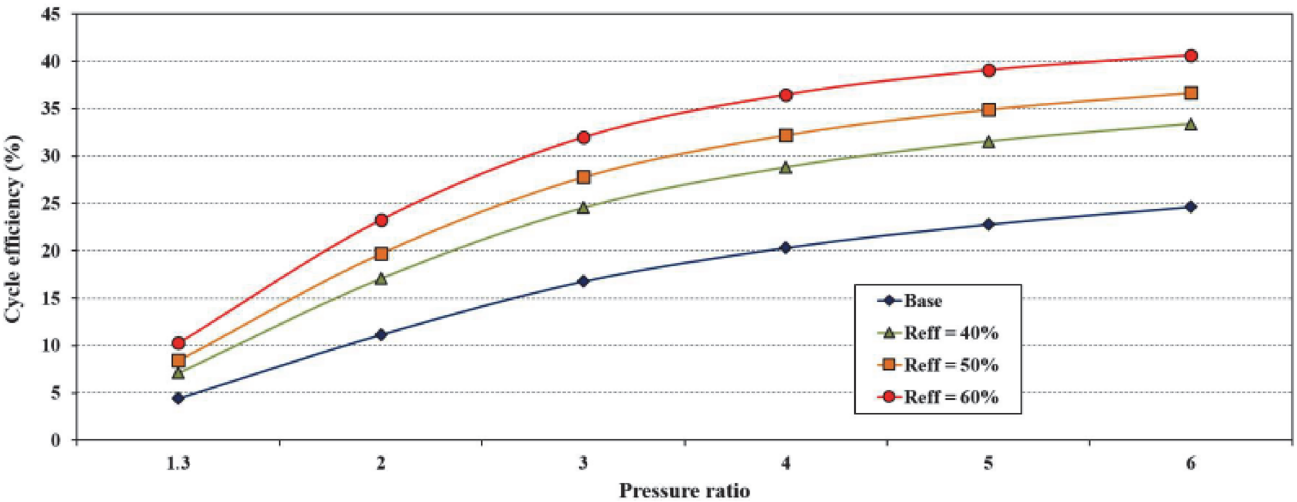

Figure 6 Cycle efficiency for the base process and for the process with regenerator at various pressure ratios

From described problem for the upgraded CO_2 closed-cycle gas turbine process it is clear why the selected heat regenerator efficiency range, taken into account in this analysis, is from 40% up to 60%.

Specific heat transferred to CO_2 in the heater for the base and upgraded CO_2 closed-cycle gas turbine processes is shown in Fig. 5

For the CO_2 closed-cycle gas turbine process upgraded with a heat regenerator, in Fig. 5 is shown that higher regenerator efficiency resulted with a lower specific heat transferred to CO_2 in the heater. Unlike base process, CO_2 closed-cycle gas turbine process upgraded with a heat regenerator shows increase in specific heat transferred to CO_2 in the heater during the increase in pressure ratio, regardless of observed regenerator efficiency.

From Fig. 6 it should be noted that the increase in pressure ratio, regardless if observing base or upgraded process, continuously increases cycle efficiency.

Base CO_2 closed-cycle gas turbine process did not reach cycle efficiency higher than 25%, even for the highest observed pressure ratio equal to 6. Such cycle efficiencies for a base process are too low for practical implementation.

CO_2 closed-cycle gas turbine process upgraded with a heat regenerator shows much higher cycle efficiencies in comparison to base process. The maximum cycle efficiency of around 40% is obtained for the pressure ratio equal to 6 and for the regenerator efficiency equal to 60%.

In order to obtain high quality regression, four MLP models are trained, two for the base process and two for the process upgraded with a heat generator. For each of these processes, specific useful work and efficiency are estimated with high values of R^2 score. Best results are achieved with the same MLP architecture for all four models which consists of three hidden layers. In the first two layers, the number of hidden neurons is 8 while in the third layer the number of hidden neurons is 32. Furthermore, *tanh* activation function is applied to hidden layers while the output layer which contains one neuron, uses the *Identity* activation function. *Adam* is used as an optimization algorithm with a learning rate of 0.01, learning rate decay of $1e^{-6}$ and $L2$ regularization parameter of $1e^{-5}$. The values of performance measure are shown in Tab. 4.

Table 4 Results of simulations for the base process and the process upgraded with a heat generator. Performance of each model is evaluated with the coefficient of determination (R^2)

CO_2 closed-cycle gas turbine process	R^2 score
Base (specific useful work)	0.99707
Upgraded with a heat regenerator (specific useful work)	0.99986
Base (efficiency)	0.99993
Upgraded with a heat regenerator (efficiency)	0.99548

According to the results presented in Tab. 4, the highest R^2 score of 0.99993 is achieved for the model used to estimate efficiency for the base process. Moreover, it can be seen that all MLP models achieved R^2 score of 0.99548 or higher, therefore, the aforementioned machine learning approach is capable for high-quality estimations in terms of thermodynamic analysis of CO_2 closed-cycle gas turbine. Similarly, Liu and Karimi (2020) demonstrate that a machine learning-based method can achieve high quality results in terms of predicting gas turbine performance for power generation [19]. In their research, Lorencin et al. (2019) use MLP for combined cycle power plant output estimation. Results show that the MLP achieves satisfactory results with RMSE value of 4.305 [9]. Fentaye et al. (2020) propose a new combined technique of ANN and Support Vector Machine for diagnostic of two-shaft industrial gas turbine engine. Results indicate that the proposed method outperforms other methods in terms of multiple fault diagnosis [20]. Park et al. (2020) demonstrate the optimized ANN for prediction of the combustor operation characteristic. Input parameters such as turbine exhaust temperature (TET) and major gas turbine design parameters are used. Based on the results, optimized architecture achieves RMSE value of 0.02296 or smaller [21].

Further research and analysis of the observed CO_2 closed-cycle gas turbine process will be performed in several directions.

Firstly, influences will be investigated of several losses on the CO_2 closed-cycle gas turbine process as for example losses through the gland seals [22], mechanical losses and additional losses related to compression or expansion processes [23], as well as other losses which can be detected inside the observed CO_2 closed-cycle gas turbine.

The other researchers also detected that CO_2 closed-cycle gas turbines can have a wide application in marine systems, especially in a waste heat recovery systems [24, 25]. From this viewpoint, it will be also of importance to perform various complex analyses of such processes by using several artificial intelligence methods [26-29].

7 CONCLUSION

This paper presents a thermodynamic analysis of CO_2 closed-cycle gas turbine which operates by using a waste heat. Two processes of such closed-cycle gas turbine are investigated - base process and the same process upgraded with a heat regenerator. The most important conclusions of the presented analysis are:

- Specific useful work is identical for both observed processes (base and upgraded). An increase in pressure ratio increases specific useful work, but only till the pressure ratio reaches the value equal to 12 (for the selected CO_2 operating parameters).
- Involving of heat regenerator inside base CO_2 closed-cycle gas turbine process requires attention due to required temperature differences necessary for the regenerator operation. It is important to note that for selected CO_2 operating parameters, high pressure ratios cannot be obtained with heat regenerator of high efficiency.
- In comparison to base CO_2 closed-cycle gas turbine process, heat regenerator operation significantly reduces specific heat transferred to CO_2 in the heater - the reduction will be as higher as regenerator has higher efficiency.
- Base CO_2 closed-cycle gas turbine process did not reach cycle efficiency higher than 25%, while for the upgraded process cycle efficiency can reach 40%.
- This analysis proves that the proposed CO_2 closed-cycle gas turbine process in practical implementation should have at least one upgrade - base process has too low cycle efficiencies for any practical implementation.
- Achieved machine learning models show high quality estimations for specific useful work and efficiency of the CO_2 closed-cycle gas turbine process. According to the obtained R^2 scores for the base and upgraded processes, such an approach is capable of estimating various CO_2 closed-cycle gas turbine output parameters.

Acknowledgements

This research has been supported by the Croatian Science Foundation under the project IP-2018-01-3739, CEEPUS network CIII-HR-0108, European Regional Development Fund under the grant KK.01.1.1.01.0009 (DATACROSS), project CEKOM under the grant KK.01.2.2.03.0004, CEI project "COVIDAi" (305.6019-20), University of Rijeka scientific grants: uniri-tehnic-18-275-1447, uniri-tehnic-18-18-1146 and uniri-tehnic-18-14.

8 REFERENCES

[1] Muše, A., Jurić, Z., Račić, N., & Radica, G. (2020). Modelling, performance improvement and emission

reduction of large two-stroke diesel engine using multi-zone combustion model. *Journal of Thermal Analysis and Calorimetry*, 1-14. https://doi.org/10.1007/s10973-020-09321-7

[2] Noor, C. M., Noor, M. M., & Mamat, R. (2018). Biodiesel as alternative fuel for marine diesel engine applications: A review. *renewable and sustainable energy reviews*, *94*, 127-142. https://doi.org/10.1016/j.rser.2018.05.031

[3] Jiaqiang, E., Zhang, Z., Chen, J., Pham, M., Zhao, X., Peng, Q., Yin, Z. et al. (2018). Performance and emission evaluation of a marine diesel engine fueled by water biodiesel-diesel emulsion blends with a fuel additive of a cerium oxide nanoparticle. *Energy Conversion and Management*, *169*, 194-205. https://doi.org/10.1016/j.enconman.2018.05.073

[4] Koroglu, T. & Sogut, O. S. (2018). Conventional and advanced exergy analyses of a marine steam power plant. *Energy*, *163*, 392-403. https://doi.org/10.1016/j.energy.2018.08.119

[5] Mrzljak, V., Blecich, P., Anđelić, N., & Lorencin, I. (2019). Energy and exergy analyses of forced draft fan for marine steam propulsion system during load change. *Journal of Marine Science and Engineering*, *7*(11), 381. https://doi.org/10.3390/jmse7110381

[6] Armellini, A., Daniotti, S., Pinamonti, P., & Reini, M. (2018). Evaluation of gas turbines as alternative energy production systems for a large cruise ship to meet new maritime regulations. *Applied energy*, *211*, 306-317. https://doi.org/10.1016/j.apenergy.2017.11.057

[7] Altosole, M., Benvenuto, G., Campora, U., Laviola, M., & Trucco, A. (2017). Waste heat recovery from marine gas turbines and diesel engines. *Energies*, *10*(5), 718. https://doi.org/10.3390/en10050718

[8] Herraiz, L., Fernández, E. S., Palfi, E., & Lucquiaud, M. (2018). Selective exhaust gas recirculation in combined cycle gas turbine power plants with post-combustion CO_2 capture. *International Journal of Greenhouse Gas Control*, *71*, 303-321. https://doi.org/10.1016/j.ijggc.2018.01.017

[9] Lorencin, I., Anđelić, N., Mrzljak, V., & Car, Z. (2019). Genetic algorithm approach to design of multi-layer perceptron for combined cycle power plant electrical power output estimation. *Energies*, *12*(22), 4352. https://doi.org/10.3390/en12224352

[10] Liu, Z. & Karimi, I. A. (2018). New operating strategy for a combined cycle gas turbine power plant. *Energy Conversion and Management*, *171*, 1675-1684. https://doi.org/10.1016/j.enconman.2018.06.110

[11] Saravanamuttoo, H. I., Rogers, G. F. C., & Cohen, H. (2001). *Gas turbine theory*. Pearson Education.

[12] Hou, S., Wu, Y., Zhou, Y., & Yu, L. (2017). Performance analysis of the combined supercritical CO2 recompression and regenerative cycle used in waste heat recovery of marine gas turbine. *Energy Conversion and Management*, *151*, 73-85. https://doi.org/10.1016/j.enconman.2017.08.082

[13] Dragunov, A. (2013). *Development of thermodynamic cycles for sodium-cooled-fast reactors*. Doctoral dissertation.

[14] Lemmon, E. W., Huber, M. L., & McLinden, M. O. (2002). NIST reference fluid thermodynamic and transport properties-REFPROP.

[15] Elsheikh, A. H., Sharshir, S. W., Abd Elaziz, M., Kabeel, A. E., Guilan, W., & Haiou, Z. (2019). Modeling of solar energy systems using artificial neural network: A comprehensive review. *Solar Energy*, *180*, 622-639. https://doi.org/10.1016/j.solener.2019.01.037

[16] Sedaghat, M. & Kiomarsiyan, A. (2019). Applying MLP-ANN as a novel and accurate method to estimate gas density. *Petroleum Science and Technology*, *37*(20), 2128-2133. https://doi.org/10.1080/10916466.2018.1482324

[17] Pontes, F. J., Amorim, G. F., Balestrassi, P. P., Paiva, A. P., & Ferreira, J. R. (2016). Design of experiments and focused grid search for neural network parameter optimization. *Neurocomputing*, *186*, 22-34. https://doi.org/10.1016/j.neucom.2015.12.061

[18] Kakac, S., Liu, H., & Pramuanjaroenkij, A. (2020). *Heat exchangers: selection, rating, and thermal design*. CRC press.

[19] Liu, Z. & Karimi, I. A. (2020). Gas turbine performance prediction via machine learning. *Energy*, *192*, 116627. https://doi.org/10.1016/j.energy.2019.116627

[20] Fentaye, A. D., Ul-Haq Gilani, S. I., Baheta, A. T., & Li, Y. G. (2019). Performance-based fault diagnosis of a gas turbine engine using an integrated support vector machine and artificial neural network method. *Proceedings of the Institution of Mechanical Engineers, Part A: Journal of Power and Energy*, *233*(6), 786-802. https://doi.org/10.1177/0957650918812510

[21] Park, Y., Choi, M., Kim, K., Li, X., Jung, C., Na, S., & Choi, G. (2020). Prediction of operating characteristics for industrial gas turbine combustor using an optimized artificial neural network. *Energy*, *213*, 118769. https://doi.org/10.1016/j.energy.2020.118769

[22] Lorencin, I., Anđelić, N., Mrzljak, V., & Car, Z. (2019). Exergy analysis of marine steam turbine labyrinth (gland) seals. *Pomorstvo*, *33*(1), 76-83. https://doi.org/10.31217/p.33.1.8

[23] Agrež, M., Avsec, J., & Strušnik, D. (2020). Entropy and exergy analysis of steam passing through an inlet steam turbine control valve assembly using artificial neural networks. *International Journal of Heat and Mass Transfer*, *156*, 119897. https://doi.org/10.1016/j.ijheatmasstransfer.2020.119897

[24] Zhang, Q., Ogren, R. M., & Kong, S. C. (2018). Thermo-economic analysis and multi-objective optimization of a novel waste heat recovery system with a transcritical CO_2 cycle for offshore gas turbine application. *Energy Conversion and Management*, *172*, 212-227. https://doi.org/10.1016/j.enconman.2018.07.019

[25] Hou, S., Zhang, F., Yu, L., Cao, S., Zhou, Y., Wu, Y., & Hou, L. (2018). Optimization of a combined cooling, heating and power system using CO_2 as main working fluid driven by gas turbine waste heat. *Energy Conversion and Management*, *178*, 235-249. https://doi.org/10.1016/j.enconman.2018.09.072

[26] Baressi Šegota, S., Lorencin, I., Anđelić, N., Mrzljak, V., & Car, Z. (2020). Improvement of Marine Steam Turbine Conventional Exergy Analysis by Neural Network Application. *Journal of Marine Science and Engineering*, *8*(11), 884. https://doi.org/10.3390/jmse8110884

[27] Štifanić, D., Musulin, J., Miočević, A., Baressi Šegota, S., Šubić, R., & Car, Z. (2020). Impact of Covid-19 on forecasting stock prices: an integration of stationary wavelet transform and bidirectional long short-term memory. *Complexity*, *2020*. https://doi.org/10.1155/2020/1846926

[28] Ali, A., Padmanaban, S., Twala, B., & Marwala, T. (2017). Electric power grids distribution generation system for optimal location and sizing - a case study investigation by various optimization algorithms. *Energies*, *10*(7), 960. https://doi.org/10.3390/en10070960

[29] Wei, Y., Hiraga, M., Ohkura, K., & Car, Z. (2019). Autonomous task allocation by artificial evolution for robotic swarms in complex tasks. *Artificial Life and Robotics*, *24*(1), 127-134. https://doi.org/10.1007/s10015-018-0466-6

Contact information:

Doc. dr. sc. Vedran MRZLJAK
(Corresponding author)
Faculty of Engineering, University of Rijeka,
Vukovarska 58, 51000 Rijeka
E-mail: vedran.mrzljak@riteh.hr

Daniel ŠTIFANIĆ, mag. ing. el.
Faculty of Engineering, University of Rijeka,
Vukovarska 58, 51000 Rijeka
E-mail: dstifanic@riteh.hr

Dr. sc. Hrvoje MEŠTRIĆ
Catolic University of Croatia,
Ilica 242, 10000 Zagreb
E-mail: hrvoje.mestric@unicath.hr

Prof. dr. sc. Zlatan CAR
Faculty of Engineering, University of Rijeka,
Vukovarska 58, 51000 Rijeka
E-mail: car@riteh.hr